Rapid Communications

Impurity moments conceal low-energy relaxation of quantum spin liquids

A. Pustogow,[1] T. Le,[1] H.-H. Wang,[1] Yongkang Luo,[1] E. Gati,[2] H. Schubert,[2] M. Lang,[2] and S. E. Brown[1]
[1]*Department of Physics and Astronomy, UCLA, Los Angeles, California 90095, USA*
[2]*Institute of Physics, Goethe University Frankfurt, 60438 Frankfurt (Main), Germany*

(Received 26 October 2019; revised manuscript received 1 February 2020; accepted 12 March 2020; published 2 April 2020)

We scrutinize the magnetic properties of κ-(BEDT-TTF)$_2$Hg(SCN)$_2$Cl through its first-order metal-insulator transition at $T_{CO} = 30$ K by means of ^{1}H nuclear magnetic resonance (NMR). While in the metallic state we find Fermi-liquid behavior with temperature-independent $(T_1T)^{-1}$, the relaxation rate exhibits a pronounced enhancement when charge order sets in. The NMR spectra remain unchanged through the transition and we find no evidence for magnetic order down to 25 mK. Similar to the isostructural spin-liquid candidates κ-(BEDT-TTF)$_2$Cu$_2$(CN)$_3$ and κ-(BEDT-TTF)$_2$Ag$_2$(CN)$_3$, T_1^{-1} acquires a dominant maximum (here around 5 K). An examination of the field dependence identifies the low-temperature feature as a dynamic inhomogeneity contribution that is typically dominant over the intrinsic relaxation but is suppressed with increasing magnetic field.

DOI: 10.1103/PhysRevB.101.140401

The rise and fall of antiferromagnetism (AFM) in correlated electron systems is intensely debated in the context of quantum spin liquids (QSLs) [1–3]. These elusive states of matter are expected to host exotic quasiparticles, such as neutral spinons or Majorana fermions, and have been advanced as possible platforms for quantum information applications. Following the original work of Anderson [4], Mott insulators on frustrated lattices are considered a natural starting point for QSL realization. In this context, insulating charge-transfer salts were among the first QSL candidate systems: the compounds κ-(BEDT-TTF)$_2$Cu$_2$(CN)$_3$ (abbreviated κ-CuCN), κ-(BEDT-TTF)$_2$Ag$_2$(CN)$_3$ (κ-AgCN), and β'-EtMe$_3$Sb[Pd(dmit)$_2$]$_2$ (β'-EtMe) are well described by anisotropic triangular-lattice models [5,6], and are observed to avoid long-range order to the lowest temperatures measured [7,8]. Consequently, the nature of the ground state, as well as the factors influencing the suppression of magnetic order have been of central importance. With respect to the former, the presence of gapless fermionic excitations has been inferred from thermodynamic probes including specific heat and spin susceptibility [9–11], as well as NMR spin-lattice relaxation [7,8,12]. In some cases, thermal transport and electrodynamic measurements [13–15] have provided evidence that these gapless excitations are also mobile [16].

The so-called κ-phase molecular solids provide a versatile playground to study the interplay of spin and charge for varying degree of electronic correlations and geometrical frustration. In the prototypical Mott insulators κ-CuCN and κ-(BEDT-TTF)$_2$Cu[N(CN)$_2$]Cl (κ-CuCl), pairs of BEDT-TTF molecules are strongly coupled [$t_d \gg t, t'$; cf. Figs. 1(a) and 1(b)], establishing a textbook-type realization of the single-band Hubbard model at 1/2 filling [5], even on quantitative scales [17]. Despite comparable exchange interaction $J/k_B \approx 200$ K, the latter compound has an AFM ground state [18], while the former exhibits no magnetic order and is therefore considered a promising QSL candidate [7,19]. Highlighting the role of frustration [1,20] in determining these disparate outcomes, despite similar structural and electronic properties, is the proposal that AFM in κ-CuCl is linked to the charge degrees of freedom [21]. That is, the detection of a dielectric anomaly [21] and pronounced phonon renormalization effects [22] close to the AFM transition were assigned to intradimer charge degrees of freedom. It was suggested [21] that charge order (CO) may reduce frustration giving rise to an ordered ground state. As well, quenched disorder [23], disorder [24–30], low dimensionality [1,31], and proximity to the Mott transition [32] have all been cited as potentially key considerations.

A promising route to disentangle the underlying mechanisms is to introduce additional symmetry breaking. Compounds comprised of the Hg-based anions [Hg(SCN)$_2X$, X = Cl, Br] have recently come into focus [33–40] due to the tendency towards electronic CO. The weaker dimerization (the ratios t_d/t and t_d/t' are closer to unity [41]) increase the relative importance of intersite Coulomb repulsion. In κ-(BEDT-TTF)$_2$Hg(SCN)$_2$Cl (κ-HgCl), the metal-insulator transition (MIT) at $T_{CO} = 30$ K is very similar to CO in α-(BEDT-TTF)$_2$I$_3$, also exhibiting a discontinuous symmetry breaking [34,35,37,42,43]. While the charge sector of κ-HgCl [33–35,40] has been investigated in great detail, no definitive conclusion was achieved on the spin degrees of freedom [33,37]. Particularly in view of the closely related κ-(BEDT-TTF)$_2$Hg(SCN)$_2$Br (κ-HgBr), where recently an exotic dipole-liquid state [39] and indications for ferromagnetism [38] were reported, the magnetic ground state and possible spin-charge coupling call for clarification.

Here we investigate the low-energy magnetic properties of κ-(BEDT-TTF)$_2$Hg(SCN)$_2$Cl via ^{1}H nuclear magnetic resonance (NMR). In the metallic phase we observe Fermi-liquid behavior with constant $(T_1T)^{-1}$ while for 25 mK $\leqslant T < T_{CO}$ spectroscopic measurements find no evidence for magnetic order. T_1^{-1} exhibits a dominant maximum around 5 K with

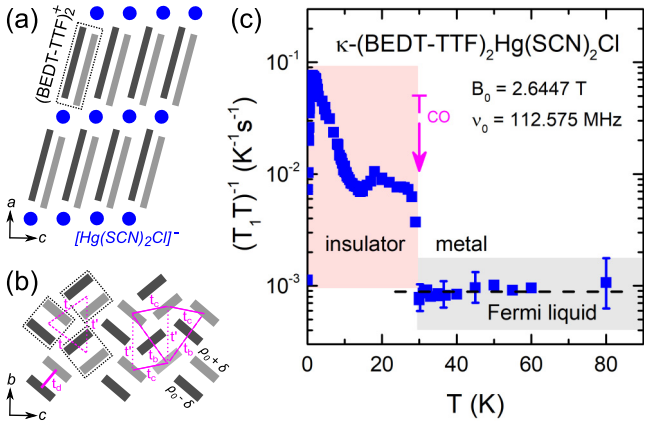

FIG. 1. (a) κ-(BEDT-TTF)$_2$Hg(SCN)$_2$Cl crystals consist of monovalent anions (blue) separating the conducting BEDT-TTF cation layers which acquire inequivalent site charges (dark and light gray) in the charge-ordered state. (b) Dimerized in-plane arrangement with a stripe pattern of charge-rich ($\rho_0 + \delta$; $\rho_0 = 0.5e$) and -poor ($\rho_0 - \delta$) molecules [34,37]. The magenta lines indicate transfer integrals t_i among (BEDT-TTF)$_2^+$ dimers (black dotted lines) and between charge-rich sites, respectively [37]. (c) In the metallic state $(T_1T)^{-1}$ is T independent, in accord with Fermi-liquid behavior [33–35]. A pronounced jump appears at the first-order MIT at T_{CO}.

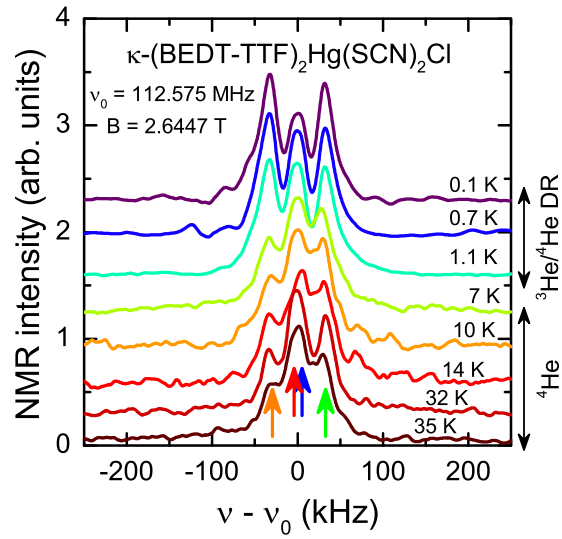

FIG. 2. The shape and width of the ^{1}H NMR spectra remain unaffected upon cooling through $T_{CO} = 30$ K, ruling out magnetic order down to millikelvin temperatures. The NMR intensity was normalized with respect to the $1/T$ enhancement; curves were shifted vertically. The minor difference in line shape below and above 2 K is due to slightly different sample alignment in the ^{3}He / ^{4}He dilution refrigerator ($T < 2$ K) and the ^{4}He flow cryostat (2–100 K) [44].

pronounced magnetic field and temperature dependencies characteristic of $S = 1/2$, $g = 2$ impurity states. Notably, the overall behavior is decidedly similar to that reported for the well-known κ-phase QSL candidates, κ-CuCN and κ-AgCN. As we will argue below, it appears that the dynamic low-temperature contribution is a common feature in all these compounds without magnetic order and originates from inhomogeneities rather than intrinsic spin degrees of freedom. We quantitatively link T_1^{-1} to impurity states detected by electron spin resonance (ESR) [33,37].

κ-(BEDT-TTF)$_2$Hg(SCN)$_2$Cl single crystals with typical dimensions of $1 \times 0.5 \times 0.3\text{mm}^3$ were grown by electrochemical methods reported elsewhere [37]. NMR experiments were performed with home-built spectrometers utilizing superconducting magnets. For sample 1, the field strength was $B_0 = 2.6447$ T, with alignment close to $\mathbf{B_0} \parallel c$. Studies of the field-dependence (sample 2; $\mathbf{B_0}$ out-of-plane) covered the range 1.2–9.3 T. Standard ^{4}He flow cryostats were employed above 1.6 K, whereas a ^{3}He / ^{4}He dilution refrigerator allowed us to access the range down to 25 mK. The spin-lattice relaxation rate was determined via free-induction decay following saturation, and analyzed using stretched-exponential fits.

The crystal structure of κ-HgCl consists of layers of positively charged BEDT-TTF molecules separated by monovalent anions [see Figs. 1(a) and 1(b)]. Within the conducting planes the organic cations are arranged in weakly bound pairs ($t_d/t' \approx 3$) assembled in an anisotropic triangular lattice ($t'/t = 0.79$ [37]), suggesting significant geometrical frustration. For $T < T_{CO}$, the electronic charge is redistributed between the two sites within a dimer, likely forming a stripelike pattern [34,37] that alters the magnetic frustration. Figure 1(c) shows the variation of $(T_1T)^{-1}$ with temperature, which is T independent in the metallic state ($T > T_{CO}$). An abrupt increase appears at the transition signaling a change of the relevant energy scale from E_F in the metal (10^3–10^4 K) to J in the insulating state (10^2 K). The nonmonotonic behavior upon further cooling will be discussed in the next paragraph. In Fig. 2 we show the ^{1}H NMR spectra for different temperatures, which appear to consist of four distinct peaks resulting from proton-proton dipolar coupling [44]. No significant modification of the peak structure is observed upon cooling below T_{CO}—clearly different from AFM in κ-CuCl [18]. Thus, the NMR spectra of κ-HgCl show no indications of magnetic order throughout the CO phase.

The spin-lattice relaxation rate T_1^{-1} is displayed on double-logarithmic scales in Fig. 3(a), covering the temperature range 0.025–80 K. For $T > T_{CO}$, the relaxation process proceeds homogeneously, as evident from the single-exponential recovery ($\alpha = 1$ in the stretched-exponential fit). Upon lowering T within the insulating state, T_1^{-1} is initially constant, falls abruptly at $T \simeq 20$ K, then increases and peaks at $T \simeq 5$ K. In this range also stretched-exponential behavior sets in [initially $\alpha \approx 0.9$; see Fig. 3(a) inset]. Well below the maximum T_1^{-1} exhibits a smooth, power-law-like decrease on cooling further to $T \sim 25$ mK, in accord with the absence of AFM concluded from the NMR spectra (Fig. 2). Stretched-exponential behavior becomes more pronounced at the lowest measured temperatures—generally an indicator for a range of characteristic relaxation time scales. In particular, $\alpha \approx 0.6$ results from a T_1^{-1} distribution spanning approximately one order of magnitude [45], which we illustrate by the red-white false-color plot behind the data in Fig. 3(a).

The low-temperature relaxation of κ-HgCl is reminiscent of the widely studied QSL candidates κ-CuCN, κ-AgCN, and β'-EtMe. In those cases, power-law variation with temperature has been attributed to a gapless continuum of spin

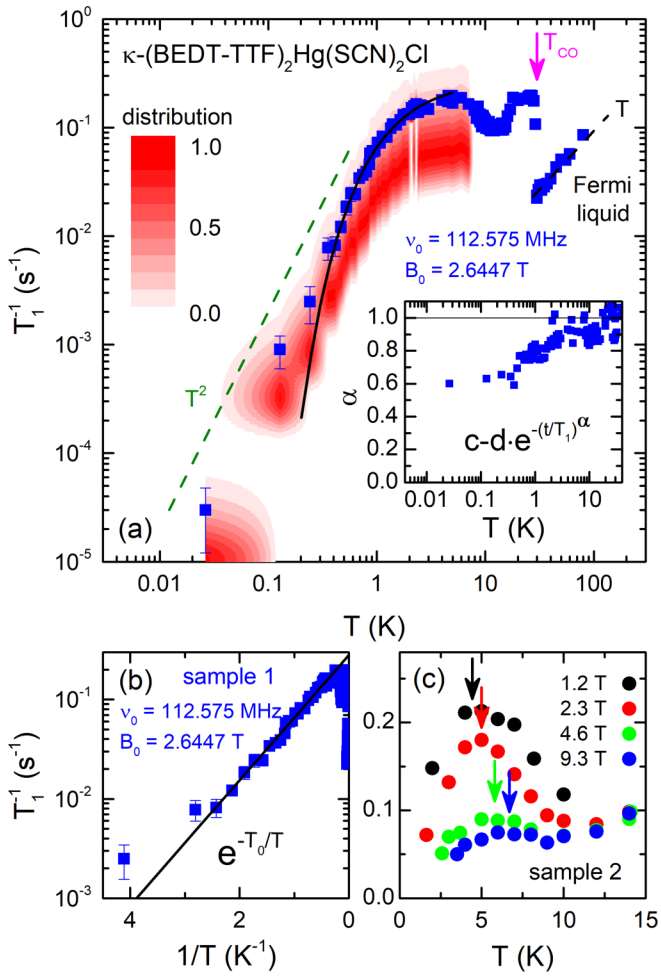

FIG. 3. (a) Subsequent to the abrupt increase at T_{CO}, the spin-lattice relaxation rate drops below 20 K, and a broad maximum forms around 5 K. Well below 1 K T_1^{-1} shows a power-law behavior similar to various spin-liquid candidates [7,12,19,46]. Inset: The stretched-exponential recovery ($\alpha = 0.6$ at lowest T) reveals a continuum of low-energy decay channels; we visualize the related distribution of T_1^{-1} (according to Ref. [45]) by the red-white false-color plot in the main graph. (b) Below the peak T_1^{-1} exhibits Arrhenius-like activation [black solid line; also indicated in (a)], with $k_B T_0 \approx \mu_B B_0$. (c) Upon increasing B_0 the maximum is strongly suppressed and shifts to higher T, in excellent agreement with Eq. (1), even in the absolute values of T_1^{-1}.

excitations [7,12,19,46]. Here, we consider an alternative scenario: the proton T_1^{-1} at low temperatures is dominated by dipolar coupling to localized $S = 1/2$, $g = 2$ spin degrees of freedom. The proposal is that the impurity spins, embedded in an otherwise nonmagnetic background, are sufficiently polarized in nonzero magnetic fields at low enough temperature, so as to progressively freeze-out this relaxation channel. We note that low-temperature effects from disorder-induced spin defects were recently considered in Ref. [30].

The nuclear relaxation by dipolar coupling to magnetic impurities implies certain behaviors that can be compared to experiment. For example, T_1^{-1} of κ-AgCN is strongly reduced with increasing B_0 [12]; similar behavior is seen for κ-HgCl in Fig. 3(c). Here the field dependence is pronounced at temperatures close to the 5 K maximum while the relaxation for $T \simeq 10$ K remains rather unaffected. At a semiquantitative level, this is precisely the temperature range corresponding to the Zeeman energy of a free spin. More specifically, the peak and low-temperature suppression of T_1^{-1} is modeled for a *single* proton as

$$T_1^{-1} = \frac{2}{5}\mu_o^2\gamma_s^2\gamma_I^2\hbar^2[S(S+1)]r^{-6}\frac{\tau}{1+\omega^2\tau^2}, \qquad (1)$$

where $1/\tau$ is the bandwidth of longitudinal field fluctuations; it is taken to be of the form $\tau = \tau_0 e^{E_Z/k_B T}$, with $E_Z = g\mu_B S B_0$ the Zeeman energy splitting of the impurity spin levels, using $g = 2$ and $S = 1/2$. The activated behavior arises from the polarization of the impurity spins in the applied magnetic field. The dipolar coupling depends on the distance r between the impurity spin and the nuclear site. Naturally, random arrangement of the former is related to a distribution of local fields which results in a stretched-exponential recovery.

Looking at the Arrhenius plot in Fig. 3(b), the behavior on the low-temperature side of the maximum closely follows the associated thermal activation with $k_B T_0 \approx \mu_B B_0$ down to 0.2 K. The peak value in Fig. 3(c) roughly follows the expected $(T_1^{-1})_{\max} \propto 1/B_0$ dependence, and $\tau = \omega^{-1}$ at the maximum yields τ_0 in the nanosecond range, in agreement with the ESR linewidth $\Delta H \approx 3$ mT in the insulating state [37]. Plugging this into Eq. (1), together with our experimental values of T_1^{-1}, yields $r \approx 6$–7 nm. A similar result is obtained from the Curie behavior of the T-dependent ESR intensity [33,37], giving an impurity concentration of order 10^{-2} per unit cell [34].

In Fig. 4(a) we compare T_1^{-1} of κ-HgCl with the isostructural QSL candidates κ-CuCN [7] and κ-AgCN [12] on common scales and for comparable B_0 as indicated. Although at different temperatures and not necessarily of the same origin, in all these compounds we identify a dynamic contribution with similar characteristics as elaborated above for κ-HgCl. Above the low-temperature maximum, $10\ \text{K} \leqslant T \leqslant 30\ \text{K}$, the data are similar in magnitude; in the case of κ-CuCN and κ-AgCN, the behavior is attributed to gapless spinons. Generally, however, the quantitative similarity across compounds is not surprising in view of the comparable exchange energies. Since the dynamic maximum dominates the low-temperature relaxation, we cannot conclude whether there is a spin gap or not. High-field experiments ($k_B T_{\max} < \mu_B B_0 < J$, i.e., a few tens of tesla) could possibly disclose the intrinsic magnetic properties of the QSL candidates down to low temperatures.

The overall suppression of the $g = 2$, $S = 1/2$ peak with increasing B_0 is similar for κ-HgCl and κ-AgCN, as summarized in Figs. 4(b) and 4(d). The published T_1^{-1} [12] on ^{1}H and ^{13}C [47] consistently show pronounced field dependence around the maximum, while the intrinsic response at higher T remains unaffected. A similar feature is also seen in the magnetic susceptibility: in the insets of (b) and (c) we show χT in order to compare to T_1^{-1} [37,48]. Similar to κ-HgCl and κ-AgCN, the ^{1}H and ^{13}C data of κ-CuCN aquired at 2 and 8.5 T [7,19], respectively, coincide above 4 K but deviate around the bump at lower T [Fig. 4(c)], where appreciable field dependence is also seen by different probes [48–50]. Due to the lack of consistent $T_1^{-1}(T)$ data upon

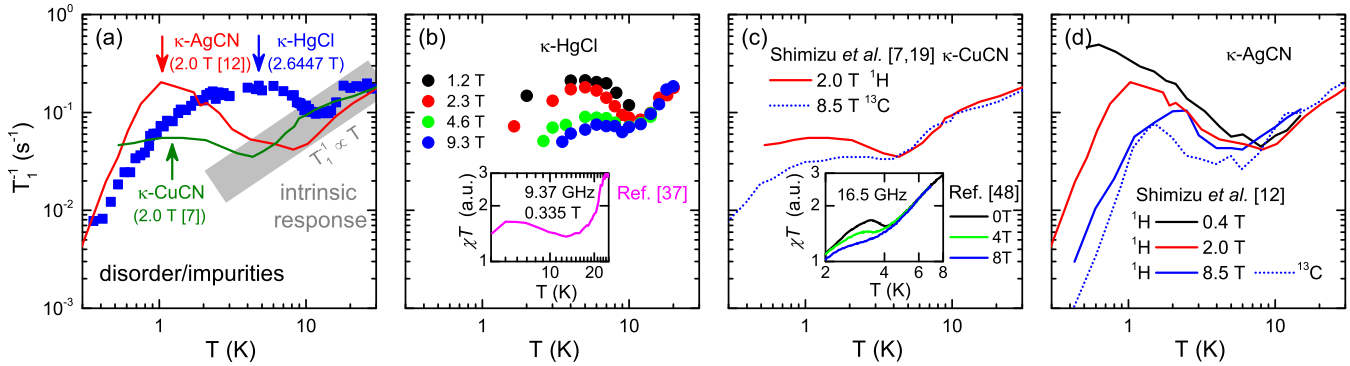

FIG. 4. (a) At temperatures above the maximum, the ^{1}H T_1^{-1} data in the insulating state of κ-HgCl coincide with the paradigmatic QSL candidates κ-CuCN and κ-AgCN. Here, T_1^{-1} follows a field-independent approximately linear T dependence suggesting that this is the intrinsic response with $J/k_B \approx 200$ K. (b)–(d) While peaked at different $T_{\max}$, the low-temperature contribution exhibits a similar suppression with higher B_0 for all three compounds; ^{13}C data (scaled by γ_n [47]) match well with the ^{1}H results acquired at the same B_0 [7,12,19]. A similar field-dependent contribution is observed in high-frequency susceptibility data plotted as χT [inset of (b) at 9.37 GHz [37]; inset of (c) at 16.5 GHz [48]].

varying B_0, we do not exclude other contributions below 4 K in κ-CuCN.

Even though the NMR characteristics of κ-HgCl resemble the response of various QSL candidates in minute detail, its thermodynamic properties clearly indicate the absence of itinerant spin and charge excitations. That is, extrapolating C/T down to $T = 0$ yields a Sommerfeld coefficient nondistinguishable from zero [39], at least much smaller than for κ-CuCN and κ-AgCN where $\gamma \approx$ 10-20 mJ K^{-2} mol^{-1} [9,12]. Note, the sister compound κ-HgBr, where fluctuating CO has been suggested [39], exhibits γ comparable to the QSL candidates. Thus, the reduced entropy in κ-HgCl is consistent with gapped charge and spin degrees of freedom, for instance if the latter resulted from a valence bond solid state below 20 K. Similar to κ-CuCN [9], C/T from Ref. [39] reveals a Schottky-like increase towards lower temperatures setting in at a few hundred millikelvin, coincident with the power law in T_1^{-1}. It remains to elucidate to what extent disorder is relevant for the material under study—in particular in view of the stretched-exponential relaxation at low temperatures that suggests a continuum of low-energy decay channels.

A similar humplike behavior with pronounced field dependence has been seen in several disordered quantum systems [51–54]. In Fig. 4 the absolute values and temperature of the maximum in T_1^{-1} differ from compound to compound. If the origins were similar, this could be associated with a varying distribution of timescales τ. Performing a similar dipolar relaxation analysis for κ-CuCN and κ-AgCN yields slightly lower impurity densities than in κ-HgCl, but of similar order of magnitude (see Supplemental Material [55], and Refs. [7,12,34,37,56–59] therein). Finally, we comment briefly on the origin of the magnetic impurities in κ-HgCl. The clearly discontinuous phase transition at 30 K allows for the possibility of multiple CO domains and accompanying domain walls, as recently observed in $(TMTTF)_2X$ by Raman spectroscopy [60]. A possible scenario is that the impurity states are located at domain walls. If that were the case, the absence of CO in κ-CuCN and κ-AgCN would point to a different origin of the dynamic contribution, likely linked to the anion layers [26,27,61]. Further, recent Raman experiments on κ-HgCl suggest BEDT-TTF$^{+0.5}$ below 20 K [40] which could also provide a source of $g = 2$, $S = 1/2$ spins.

To summarize, we map the low-energy spin dynamics in κ-(BEDT-TTF)$_2$Hg(SCN)$_2$Cl through the metal-insulator transition by comprehensive ^{1}H NMR experiments. The spin-lattice relaxation rate indicates a Fermi-liquid metal at elevated temperatures, and exhibits a pronounced discontinuous increase upon cooling through $T_{\rm CO} = 30$ K into the charge-ordered phase. From the unaltered NMR spectra (Fig. 2) and the smooth temperature dependence of T_1^{-1} upon $T \to 0$ (Fig. 3), we conclude the absence of long-range magnetic order. Notably, we find that the magnetic response is essentially identical to isostructural QSL candidates [7,12,19], including the stretched-exponential recovery and a power-law-like tail well below 1 K as well as a pronounced maximum in T_1^{-1} (peaked around 5 K in κ-HgCl). This low-T contribution exhibits a strong field dependence, very similar for κ-HgCl and κ-AgCN, likely originating from dipolar coupling to impurity spins. Taken together, these results imply that the low-temperature NMR properties in all these frustrated materials [7,12,19,46] are dominated by extrinsic magnetic contributions. Suppressing the dynamic relaxation channels with high fields ($B_0 \geqslant 10$ T) may recover the intrinsic electronic response, providing a promising route to answer the question about a spin gap in the triangular systems. Given the lack of a nonzero fermionic contribution to the low-temperature specific heat [39], the case for a spin-gapped ground state, with the gap opening at $T \simeq 20$ K, is stronger for κ-HgCl than it is for κ-CuCN and κ-AgCN.

We thank N. Drichko, K. Kanoda, R. Valentí, S. Winter, M. Dressel, and A.-M. Tremblay for useful comments and discussions. A.P. acknowledges support by the Alexander von Humboldt Foundation through the Feodor Lynen Fellowship. This work was supported by the National Science Foundation (DMR-1709304). Work performed in Frankfurt was supported by the Deutsche Forschungsgemeinschaft through the Transregional Collaborative Research Center SFB/TR49.

[1] L. Balents, Nature (London) **464**, 199 (2010).
[2] L. Savary and L. Balents, Rep. Prog. Phys. **80**, 016502 (2017).
[3] Y. Zhou, K. Kanoda, and T.-K. Ng, Rev. Mod. Phys. **89**, 025003 (2017).
[4] P. W. Anderson, Mater. Res. Bull. **8**, 153 (1973).
[5] H. Kino and H. Fukuyama, J. Phys. Soc. Jpn. **65**, 2158 (1996).
[6] R. Kato, Chem. Rev. **104**, 5319 (2004).
[7] Y. Shimizu, K. Miyagawa, K. Kanoda, M. Maesato, and G. Saito, Phys. Rev. Lett. **91**, 107001 (2003).
[8] T. Itou, A. Oyamada, S. Maegawa, M. Tamura, and R. Kato, Phys. Rev. B **77**, 104413 (2008).
[9] S. Yamashita, Y. Nakazawa, M. Oguni, Y. Oshima, H. Nojiri, Y. Shimizu, K. Miyagawa, and K. Kanoda, Nat. Phys. **4**, 459 (2008).
[10] S. Yamashita, T. Yamamoto, Y. Nakazawa, M. Tamura, and R. Kato, Nat. Commun. **2**, 275 (2011).
[11] D. Watanabe, M. Yamashita, S. Tonegawa, Y. Oshima, H. M. Yamamoto, R. Kato, I. Sheikin, K. Behnia, T. Terashima, S. Uji, T. Shibauchi, and Y. Matsuda, Nat. Commun. **3**, 1090 (2012).
[12] Y. Shimizu, T. Hiramatsu, M. Maesato, A. Otsuka, H. Yamochi, A. Ono, M. Itoh, M. Yoshida, M. Takigawa, Y. Yoshida, and G. Saito, Phys. Rev. Lett. **117**, 107203 (2016).
[13] M. Yamashita, N. Nakata, Y. Senshu, M. Nagata, H. M. Yamamoto, R. Kato, T. Shibauchi, and Y. Matsuda, Science **328**, 1246 (2010).
[14] M. Dressel and A. Pustogow, J. Phys.: Condens. Matter **30**, 203001 (2018).
[15] A. Pustogow, Y. Saito, E. Zhukova, B. Gorshunov, R. Kato, T.-H. Lee, S. Fratini, V. Dobrosavljević, and M. Dressel, Phys. Rev. Lett. **121**, 056402 (2018).
[16] The results from Ref. [13] have been recently challenged in Ref. [62].
[17] A. Pustogow, M. Bories, A. Löhle, R. Rösslhuber, E. Zhukova, B. Gorshunov, S. Tomić, J. A. Schlueter, R. Hübner, T. Hiramatsu, Y. Yoshida, G. Saito, R. Kato, T.-H. Lee, V. Dobrosavljević, S. Fratini, and M. Dressel, Nat. Mater. **17**, 773 (2018).
[18] K. Miyagawa, A. Kawamoto, Y. Nakazawa, and K. Kanoda, Phys. Rev. Lett. **75**, 1174 (1995).
[19] Y. Shimizu, K. Miyagawa, K. Kanoda, M. Maesato, and G. Saito, Phys. Rev. B **73**, 140407(R) (2006).
[20] H. C. Kandpal, I. Opahle, Y.-Z. Zhang, H. O. Jeschke, and R. Valentí, Phys. Rev. Lett. **103**, 067004 (2009); K. Nakamura, Y. Yoshimoto, T. Kosugi, R. Arita, and M. Imada, J. Phys. Soc. Jpn. **78**, 83710 (2009).
[21] P. Lunkenheimer, J. Müller, S. Krohns, F. Schrettle, A. Loidl, B. Hartmann, R. Rommel, M. de Souza, C. Hotta, J. A. Schlueter, and M. Lang, Nat. Mater. **11**, 755 (2012).
[22] M. Matsuura, T. Sasaki, S. Iguchi, E. Gati, J. Müller, O. Stockert, A. Piovano, M. Böhm, J. T. Park, S. Biswas, S. M. Winter, R. Valentí, A. Nakao, and M. Lang, Phys. Rev. Lett. **123**, 027601 (2019).
[23] D. Guterding, R. Valentí, and H. O. Jeschke, Phys. Rev. B **92**, 081109(R) (2015).
[24] D. A. Huse and V. Elser, Phys. Rev. Lett. **60**, 2531 (1988).
[25] T. Furukawa, K. Miyagawa, T. Itou, M. Ito, H. Taniguchi, M. Saito, S. Iguchi, T. Sasaki, and K. Kanoda, Phys. Rev. Lett. **115**, 077001 (2015).
[26] M. Dressel, P. Lazić, A. Pustogow, E. Zhukova, B. Gorshunov, J. A. Schlueter, O. Milat, B. Gumhalter, and S. Tomić, Phys. Rev. B **93**, 081201(R) (2016).
[27] M. Pinterić, D. Rivas Góngora, Ž. Rapljenović, T. Ivek, M. Čulo, B. Korin-Hamzić, O. Milat, B. Gumhalter, P. Lazić, M. Sanz Alonso, W. Li, A. Pustogow, G. Gorgen Lesseux, M. Dressel, and S. Tomić, Crystals **8**, 190 (2018).
[28] T. Itou, E. Watanabe, S. Maegawa, A. Tajima, N. Tajima, K. Kubo, R. Kato, and K. Kanoda, Sci. Adv. **3**, e1601594 (2017).
[29] P. Lazić, M. Pinterić, D. Rivas Góngora, A. Pustogow, K. Treptow, T. Ivek, O. Milat, B. Gumhalter, N. Došlić, M. Dressel, and S. Tomić, Phys. Rev. B **97**, 245134 (2018).
[30] K. Riedl, R. Valentí, and S. M. Winter, Nat. Commun. **10**, 2561 (2019).
[31] B. J. Powell, E. P. Kenny, and J. Merino, Phys. Rev. Lett. **119**, 087204 (2017).
[32] O. I. Motrunich, Phys. Rev. B **72**, 045105 (2005).
[33] S. Yasin, E. Rose, M. Dumm, N. Drichko, M. Dressel, J. A. Schlueter, E. I. Zhilyaeva, S. Torunova, and R. N. Lyubovskaya, Physica B: Condens. Matter **407**, 1689 (2012).
[34] N. Drichko, R. Beyer, E. Rose, M. Dressel, J. A. Schlueter, S. A. Turunova, E. I. Zhilyaeva, and R. N. Lyubovskaya, Phys. Rev. B **89**, 075133 (2014).
[35] A. Löhle, E. Rose, S. Singh, R. Beyer, E. Tafra, T. Ivek, E. I. Zhilyaeva, R. N. Lyubovskaya, and M. Dressel, J. Phys.: Condens. Matter **29**, 055601 (2017).
[36] T. Ivek, R. Beyer, S. Badalov, M. Čulo, S. Tomić, J. A. Schlueter, E. I. Zhilyaeva, R. N. Lyubovskaya, and M. Dressel, Phys. Rev. B **96**, 085116 (2017).
[37] E. Gati, J. K. H. Fischer, P. Lunkenheimer, D. Zielke, S. Köhler, F. Kolb, H.-A. K. von Nidda, S. M. Winter, H. Schubert, J. A. Schlueter, H. O. Jeschke, R. Valentí, and M. Lang, Phys. Rev. Lett. **120**, 247601 (2018).
[38] M. Hemmida, H.-A. Krug von Nidda, B. Miksch, L. L. Samoilenko, A. Pustogow, S. Widmann, A. Henderson, T. Siegrist, J. A. Schlueter, A. Loidl, and M. Dressel, Phys. Rev. B **98**, 241202(R) (2018).
[39] N. Hassan, S. Cunningham, M. Mourigal, E. I. Zhilyaeva, S. A. Torunova, R. N. Lyubovskaya, J. A. Schlueter, and N. Drichko, Science **360**, 1101 (2018).
[40] N. M. Hassan, K. Thirunavukkuarasu, Z. Lu, D. Smirnov, E. I. Zhilyaeva, S. Torunova, R. N. Lyubovskaya, and N. Drichko, npj Quantum Mater. **5**, 15 (2020).
[41] While for κ-(BEDT-TTF)$_2$Hg(SCN)$_2$Cl $t_d/t' \approx 3$, the paradigmatic κ-phase materials κ-CuCN, κ-AgCN, and κ-CuCl have larger ratios of approximately 4–5.
[42] Y. Yue, K. Yamamoto, M. Uruichi, C. Nakano, K. Yakushi, S. Yamada, T. Hiejima, and A. Kawamoto, Phys. Rev. B **82**, 075134 (2010).
[43] T. Ivek, B. Korin-Hamzić, O. Milat, S. Tomić, C. Clauss, N. Drichko, D. Schweitzer, and M. Dressel, Phys. Rev. B **83**, 165128 (2011).
[44] The spectrum is actually comprised of a superposition of eight inequivalent but unresolved proton sites. See Supplemental Material for angle-dependent measurements [55].
[45] D. C. Johnston, Phys. Rev. B **74**, 184430 (2006).
[46] T. Itou, A. Oyamada, S. Maegawa, and R. Kato, Nat. Phys. **6**, 673 (2010).

[47] Upon proper renormalization to the gyromagnetic ratios and the local charge density [cf. Fig. 4(a) in Ref. [12]], the ^{1}H and ^{13}C data coincide in the relevant temperature range ($k_BT \leqslant J$) when acquired at the same magnetic field. Upon changing B_0, the apparently intrinsic response at temperatures above the maximum remains unaltered, while the low-T behavior exhibits pronounced modifications, including suppression by field [12].

[48] M. Poirier, S. Parent, A. Côté, K. Miyagawa, K. Kanoda, and Y. Shimizu, Phys. Rev. B **85**, 134444 (2012).

[49] F. L. Pratt, P. J. Baker, S. J. Blundell, T. Lancaster, S. Ohira-Kawamura, C. Baines, Y. Shimizu, K. Kanoda, I. Watanabe, and G. Saito, Nature (London) **471**, 612 (2011).

[50] T. Isono, T. Terashima, K. Miyagawa, K. Kanoda, and S. Uji, Nat. Commun. **7**, 13494 (2016); T. Isono, S. Sugiura, T. Terashima, K. Miyagawa, K. Kanoda, and S. Uji, *ibid.* **9**, 1509 (2018).

[51] B. J. Suh, P. C. Hammel, M. Hücker, B. Büchner, U. Ammerahl, and A. Revcolevschi, Phys. Rev. B **61**, R9265 (2000).

[52] M. Klanjšek, A. Zorko, R. Žitko, J. Mravlje, Z. Jagličić, P. K. Biswas, P. Prelovšek, D. Mihailovic, and D. Arčon, Nat. Phys. **13**, 1130 (2017).

[53] F. Hammerath, R. Sarkar, S. Kamusella, C. Baines, H.-H. Klauss, T. Dey, A. Maljuk, S. Gaß, A. U. B. Wolter, H.-J. Grafe, S. Wurmehl, and B. Büchner, Phys. Rev. B **96**, 165108 (2017).

[54] K. Kitagawa, T. Takayama, Y. Matsumoto, A. Kato, R. Takano, Y. Kishimoto, S. Bette, R. Dinnebier, G. Jackeli, and H. Takagi, Nature (London) **554**, 341 (2018).

[55] See Supplemental Material at http://link.aps.org/supplemental/10.1103/PhysRevB.101.140401 for details on the impurity density approximation from spin susceptibility utilizing Curie law, NMR spectra upon rotation, and nuclear magnetization recovery.

[56] H. O. Jeschke, M. de Souza, R. Valentí, R. S. Manna, M. Lang, and J. A. Schlueter, Phys. Rev. B **85**, 035125 (2012).

[57] T. Hiramatsu, Y. Yoshida, G. Saito, A. Otsuka, H. Yamochi, M. Maesato, Y. Shimizu, H. Ito, Y. Nakamura, H. Kishida, M. Watanabe, and R. Kumai, Bull. Chem. Soc. Jpn. **90**, 1073 (2017).

[58] A. Abragam, *Principles of Nuclear Magnetism* (Oxford University Press, Hong Kong, 1983).

[59] E. Gati, S. M. Winter, J. A. Schlueter, H. Schubert, J. Müller, and M. Lang, Phys. Rev. B **97**, 075115 (2018).

[60] R. Świetlik, B. Barszcz, A. Pustogow, and M. Dressel, Phys. Rev. B **95**, 085205 (2017).

[61] K. G. Padmalekha, M. Blankenhorn, T. Ivek, L. Bogani, J. A. Schlueter, and M. Dressel, Phys. B (Amsterdam, Neth.) **460**, 211 (2015).

[62] P. Bourgeois-Hope, F. Laliberté, E. Lefrançois, G. Grissonnanche, S. R. de Cotret, R. Gordon, S. Kitou, H. Sawa, H. Cui, R. Kato, L. Taillefer, and N. Doiron-Leyraud, Phys. Rev. X **9**, 041051 (2019).